Link optimization for DWDM transmission with an optical phase conjugation

Research Article | Vol. 24, No. 15 / 25 Jul 2016 / OPTICS EXPRESS 16450

Optics EXPRESS

Link optimization for DWDM transmission with an optical phase conjugation

PAWEŁ ROSA,* GIUSEPPE RIZZELLI, AND JUAN DIEGO ANIA-CASTAÑÓN

Instituto de Óptica, Consejo Superior de Investigaciones Cientificas, Madrid 28006, Spain
**p.g.rosa@icloud.com*

Abstract: We characterize in-span signal power asymmetry in random distributed feedback ultralong Raman laser-amplified WDM transmission and numerically optimize fiber span length and operating band to achieve the lowest inter-span signal power asymmetry between transmitted and optically conjugated channels in systems relying upon mid-link optical conjugation to combat fiber nonlinear impairments.

OCIS codes: (060.1660) Coherent communications; (060.2320) Fibre optics amplifiers and oscillators; (060.4370) Nonlinear optics, fibers.

References and links

1. P. P. Mitra and J. B. Stark, "Nonlinear limits to the information capacity of optical fiber communications," Nature, **411**, 1027–1030 (2001).
2. A. D. Ellis, J. Zhao, and D. Cotter, "Approaching the Non-Linear Shannon Limit," J. Light. Tech. **28**(4), 423–433 (2010).
3. I. R. Gabitov and P. M. Lushnikov, "Nonlinearity management in a dispersion-managed system," Opt. Lett. **27**(2), 113–115 (2002).
4. J. D. Ania-Castañòn, I.O. Nasieva, N. Kurukitkoson, S.K. Turitsyn, C. Borsier, and E. Pincemin, "Nonlinearity management in fiber transmission systems with hybrid amplification," Opt. Commun. **233**(4–6), 353–357 (2004).
5. A. J. Lowery, "Fiber nonlinearity pre- and post-compensation for long-haul optical links using OFDM," Opt. Express **15**(20), 12965–12970 (2007).
6. E. Ip and J. M. Kahn, "Compensation of dispersion and nonlinear impairments using digital backpropagation," J. Light. Tech., **26**(20), 3416–3425 (2008).
7. S. Watanabe, and M. Shirasaki, "Exact compensation for both chromatic dispersion and Kerr effect in a transmission fiber using optical phase conjugation," J. Light. Tech. **14**(3), 243–248 (1996).
8. P. Minzioni, I. Cristiani, V. Degiorgio, L. Marazzi, M. Martinelli, C. Langrock, and M. M. Fejer, "Experimental demonstration of nonlinearity and dispersion compensation in an embedded link by optical phase conjugation," Phot. Tech. Lett. **18**(9), 995–997 (2006).
9. D. Rafique, J. Zhao, and A. D. Ellis, "Digital back-propagation for spectrally efficient WDM 112 Gbit/s PM m-ary QAM transmission," Opt. Express **19**(6), 5219–5224 (2011).
10. E. Temprana, E. Myslivets, B.P.-P. Kuo, L. Liu, V. Ataie, N. Alic, S. Radic, "Overcoming Kerr-induced capacity limit in optical fiber transmission," Science 26, **348**(6242), 1445–1448 (2015).
11. S. L. Jansen, D. van den Borne, G. D. Khoe, H. de Waardt, P. M. Krummrich, and S. Spalter, "Phase conjugation for increased system robustness," in Optical Fiber Communication Conference and Exposition and The National Fiber Optic Engineers Conference, Technical Digest (CD) (Optical Society of America, 2006), paper OTuK3.
12. M. D. Pelusi and B. J. Eggleton, "Optically tunable compensation of nonlinear signal distortion in optical fiber by end-span optical phase conjugation," Opt. Express **20**(7), 8015–8023 (2012).
13. I. D. Phillips, M. Tan, M.F.C. Stephens, M. McCarthy, E. Giacoumidis, S. Sygletos, P. Rosa, S. Fabbri, S. T. Le, T. Kanesan, S. K. Turitsyn, N. J. Doran, and A. D. Ellis, "Exceeding the nonlinear Shannon limit using Raman fiber based amplification and optical phase conjugation," in Optical Fiber Communication Conference, OSA Technical Digest (online) (Optical Society of America, 2014), paper M3C.1.
14. M. Tan, P. Rosa, I. D. Phillips, and P. Harper, "Extended Reach of 116 Gb/s DP-QPSK Transmission using Random DFB Fiber Laser Based Raman Amplification and Bidirectional Second-order Pumping," in Optical Fiber Communication Conference, OSA Technical Digest (online) (Optical Society of America, 2015), paper W4E.1.
15. P. Rosa, G. Rizzelli, M. Tan, P. Harper, and J. D. Ania-Castañòn, "Characterisation of random DFB Raman laser amplifier for WDM transmission," Opt. Express **23**(22), 28634–28639 (2015).
16. M. Tan, P. Rosa, S. T. Le, Md. A. Iqbal, I. D. Phillips, and P. Harper, "Transmission performance improvement using random DFB laser based Raman amplification and bidirectional second-order pumping," Opt. Express **24**(3), 2215–2221 (2016).

#264830 http://dx.doi.org/10.1364/OE.24.016450
Journal © 2016 Received 10 May 2016; revised 28 Jun 2016; accepted 29 Jun 2016; published 12 Jul 2016

Optics EXPRESS

17. P. Rosa, G. Rizzelli, and J. D. Ania-Castañón, "Signal power symmetry optimization for optical phase conjugation using Raman amplification," in *Proceedings of Nonlinear Optics*, OSA Technical Digest (online) (Optical Society of America, 2015), paper NW4A.36.
18. P. Rosa, S. T. Le, G. Rizzelli, M. Tan, and J. D. Ania-Castañón, "Signal power asymmetry optimization for optical phase conjugation using Raman amplification," Opt. Express **23**(25), 31772–31778 (2015).
19. S. K. Turitsyn, S. A. Babin, A. E. El-Taher, P. Harper, D. V. Churkin, S. I. Kablukov, J. D. Ania-Castañón, V. Karalekas, E. V. Podivilov, "Random distributed feedback fiber laser," Nature Photonics **4**, 231–235, (2010).
20. M. Alcon-Camas, A. E. El-Taher, J. D. Ania-Castañón, and P. Harper, "Gain Bandwidth Optimisation and Enhancement in Ultra-long Raman Fibre Laser based Amplifiers," in European Conference and Exhibition on Optical Communication (ECOC), (IEEE, 2010), paper P1.17.
21. M. Tan, P. Rosa, Md. A. Iqbal, I. D. Phillips, J. D. Ania-Castañón and P. Harper, "RIN Mitigation in Second Order Pumped Raman Fibre Laser Based Amplification," in Asia Communications and Photonics Conference, (OSA 2015), paper AM2E.6.
22. C. R. S. Fludger, V. Handerek and R. J. Mears, "Pump to Signal RIN Transfer in Raman Fiber Amplifiers," J. Light. Tech. **19**(8), (2001).
23. M. Tan, P. Rosa, I. D. Phillips, and P. Harper, "Long-haul Transmission Performance Evaluation of Ultra-long Raman Fiber Laser Based Amplification Influenced by Second Order Co-pumping," in Asia Communications and Photonics Conference, OSA Technical Digest (online) (Optical Society of America, 2014), paper ATh1E.4.
24. M. Tan, P. Rosa, S. T. Le, I. D. Phillips, and P. Harper, "Evaluation of 100G DP-QPSK long-haul transmission performance using second order co-pumped Raman laser based amplification," Opt. Express **23**(17), 22181-22189 (2015).
25. J. D. Ania-Castañón, "Quasi-lossless transmission using second-order Raman amplification and fiber Bragg gratings," Opt. Express **12**(19), 4372-4377 (2004).
26. K. Solis-Trapala, T. Inoue, and S. Namiki, "Signal power asymmetry tolerance of an optical phase conjugation-based nonlinear compensation system," in European Conference and Exhibition on Optical Communication (ECOC), (IEEE, 2014), paper We.2.5.4

1. Introduction

The nonlinear-Shannon limit sets a cap to the maximum capacity in single mode optical fibers [1, 2]. Several techniques have been proposed over the years to compensate or partially mitigate fiber nonlinear effects, such as pre-shaping and in-line nonlinearity management [3–6], dispersion engineered transmission systems with optical phase conjugation (OPC) [7, 8] or digital compensation through techniques such as back-propagation [6, 9, 10]. Amongst these options, mid-link [11] or transmitter-based [12] OPC has proven to be one of the most promising, enabling real time compensation of all deterministic (signal$\times$signal) nonlinear impairments [13] in systems similar to those already installed. However, the degree of nonlinear compensation using mid-link OPC without the addition of dispersion engineering depends on the symmetry match of the conjugated and transmitted signal power evolution in the fiber. Meaningful signal power symmetry improvement over standard fibers has been demonstrated in fiber-optic links with Raman-based distributed amplification, with the additional advantage of an improved noise performance. A simple approach to improve performance in mid-link OPC-assisted systems while retaining a periodic span structure lies in reducing signal power asymmetry within the periodic spans themselves, while ensuring a low impact of noise and non-deterministic nonlinear impairments in the overall transmission link. This approach assumes in-span signal evolution to be the same before and after conjugation, which will be valid only for small frequency shifts of the conjugated signal. It has been demonstrated that a novel half-open-cavity random distributed feedback (DFB) Raman laser amplifier with bidirectional 2nd order pumping [14–16] can reduce in-span asymmetry with respect to its middle point and shows the highest level of in-span symmetry achieved up to date [17, 18].

Here, in order to investigate the best practical Raman-based link design for OPC, we take into account for the first time the potential impact of conjugated signal frequency shift on inter-span asymmetry between transmitted and conjugated channels in multi wavelength transmission (WDM), considering 5 different frequency sections across the C-band (192 - 195.775 THz). Each section consists of two WDM grids (original and conjugated) of 20 channels with a 25 GHz spacing that are simulated independently. We also show the optimized single channel in-span

Optics EXPRESS

signal power asymmetry variation due to wavelength dependent Raman gain and attenuation at different frequencies and span lengths.

2. Amplification setup

Fig. 1. Schematic design of random DFB Raman laser amplifier.

In our search for an optimal setup for WDM transmission with an OPC we consider random DFB Raman fiber laser amplifier [14, 15] as it shows the best in-span asymmetry performance comparing with other Raman amplification schemes [17, 18]. The schematic design is shown in Fig. 1. To form a distributed 2nd order random DFB Raman laser amplifier, fully depolarized Raman fiber laser pumps are downshifted in wavelength by two Stokes with respect to the frequency of the signal. High reflectivity (99%) FBG centered at 1455 nm with a 200 GHz bandwidth was deployed at the end of the transmission line to reflect Stokes-shifted light from the backward pump at 1366 nm and form a random DFB lasing [19] at the frequency specified by the wavelength of the FBG acting as a first order pump that amplified the signal in the C-band. The advantage of this model is that the gain bandwidth and profile can be modified by selecting appropriate FBG [20] rather than deploying a seed at different wavelength. The lack of an FBG on the side of the forward pump reduces the RIN transfer [21] from the forward pump to the Stokes-shifted light at 1455 nm at the cost of a reduction in the power efficiency conversion in comparison to the 1st order Raman and URFL amplification schemes. This is particularly important, as forward-pumping RIN transfer from inherently noisy high-power pumps can seriously hinder data transmission [22–24].

As was shown in [18], for the proposed amplificatipon setup and with up to 42 channels located in the C-band, in-span asymmetry is pretty much independent of input signal power as long as the power per channel is below 0 dBm. Unless otherwise stated, the channel power used in our simulations was -5 dBm.

3. Wavelength dependent in-span asymmetry

To show wavelength dependent in-span asymmetry we numerically obtain the average power profiles of a single channel sweeping the wavelength across the 30 nm C-band (1531 - 1561 nm) with a 25 GHz step. Our broadband amplification model includes not only cascaded amplification, but also takes into account residual Raman gain from the primary pump at 1366 nm to the signal in the C-band, pump depletion from both pumps to the lower order pumps and signal components, double Rayleigh scattering and amplified spontaneous emission noise for each of the signals. The full description of the extended model used as well as parameters (attenuation curve at different frequencies, Rayleigh backscattering and Raman gain coefficients) for standard SMF-28 fiber used in the simulations can be found in [15]. The in-span signal power asymmetry was determined as in [26]:

$$Asymmetry = \frac{\int_0^{L/2} |P(z) - P(L-z)| dz}{\int_0^{L/2} P(z) dz} \times 100 \quad (1)$$

where L is the span length and P represents average signal power evolution within the span.

The simulated span length ranged from 50 - 70 km. The pumps were optimized to give 0 dBm net gain and the lowest in-span asymmetry at each distance. Pump powers will depend on the fiber type, more specifically on the combination of three factors: Raman gain coefficient and the attenuation coefficients at the pumping wavelength and the wavelength of the FBG used, however,

Optics EXPRESS

the optimal forward pump power will remain constant and the pumps ratio will be driven mainly by increasing backward pump needed to recover the signal at the end of the span. In Fig. 2(a) we plot the forward pump power split (% forward to total pump power) at the central frequency (1546 nm) and the forward and backward pump powers versus span length. With longer spans the optimal forward pump is almost constant whereas the backward pump increases. The signal at different frequency with the combination of the Raman gain will experience different effective loss, hence the ratio pumps ratio will vary, respectively. This is illustrated in Fig. 2(b) where we plot pump ratios at 50, 60 and 70 km versus frequency.

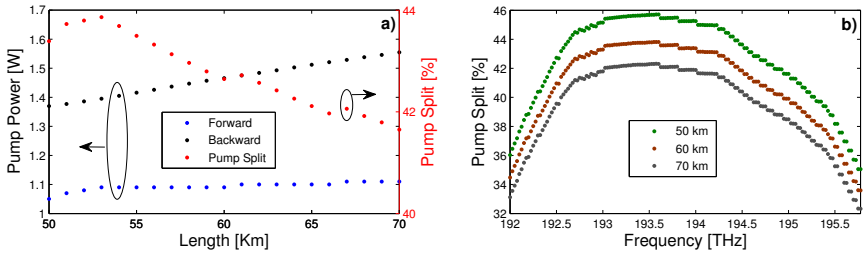

Fig. 2. Dependence of asymmetry, measured at 1545 nm in a 60 km span, on the forward pump power split.

In Fig. 3 we compare the experimentally measured asymmetry vs. forward pump power split to the simulated predictions for a signal wavelength of 1545 nm in a 60 km span. The discrepancies between the measured and simulated results can be attributed to noisy experimental power profiles as well as a minor Raman gain and attenuation coefficients mismatch (for consistency with previous simulations we used standard values for SMF-28 fiber rather than measured coefficients).

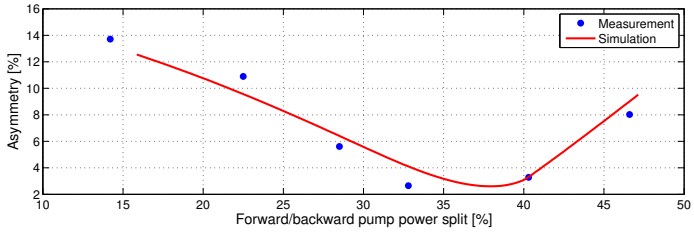

Fig. 3. Asymmetry dependence on the forward pump power split measured at the central wavelength at 1545 nm in a 60 km span.

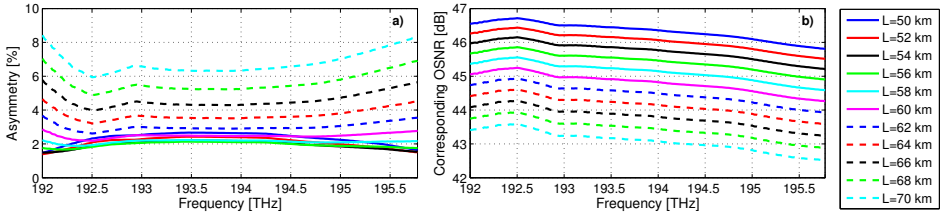

Fig. 4. In-span signal power asymmetry of a single channel at given frequency for different span lengths (a) and corresponding OSNR (b).

Higher order Raman amplification can push the gain further into the span [25] allowing better control over average power distribution of the signal. With fixed fiber parameters, a second order random DFB Raman amplifier will have controllable asymmetry only up to a certain maximum length, beyond which gain in the two halves of the span can not be balanced. To reduce asymmetry with longer span lengths would require, for example, to devise spans with lower attenuation in their second half.

Optics EXPRESS

In Fig. 4 we show the lowest in-span asymmetry of a single channel and its corresponding OSNR at a given frequency for each distance considered. With longer spans, the in-span asymmetry variation of a single channel across the residual grid is more pronounced. This variation is mainly due to Raman gain coefficient that is lower at the residual frequencies. The flattest asymmetry response and lowest overall in-span asymmetry excursion, calculated as the difference between the asymmetry of the best and worst performing channels across the simulated band, was found at 58 km span length (Fig. 5), for which the asymmetry variation was less than 0.4 %.

The optimization of the link for the wide-band WDM data transmission is important as the performance of an OPC is directly related to the symmetry of the transmitted and conjugated channel. Span lengths below 62 km offer the lowest in-span asymmetry as well as asymmetry excursion across the measured band (solid curves in Fig. 4[a]), hence further optimization for WDM transmission was performed in that region.

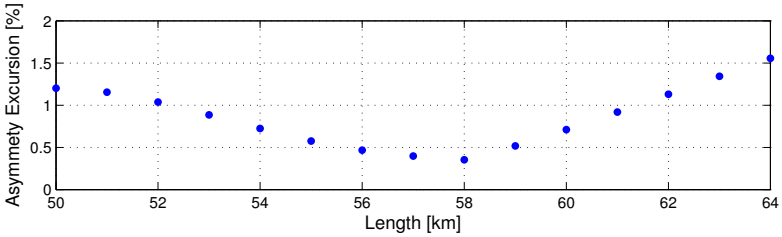

Fig. 5. Asymmetry excursion of the power profiles within a span between the best and the worst performing channel across C-band (1531-1561 nm). Results are based on Fig. 4(a).

4. DWDM transmission with a mid-link OPC

In DWDM transmission with a mid-link OPC we independently simulate the power evolution of the original channels and their conjugated copies, that are shifted in frequency. The channel count was set to 20, with a 25 GHz spacing. We assumed 300 GHz spacing for the optical phase conjugator. The grid was then downshifted in wavelength by 500 GHz until the 30 nm band (1531 - 1561 nm) was fully covered. A diagram depicting the simulated frequency sections is shown in Fig. 6.

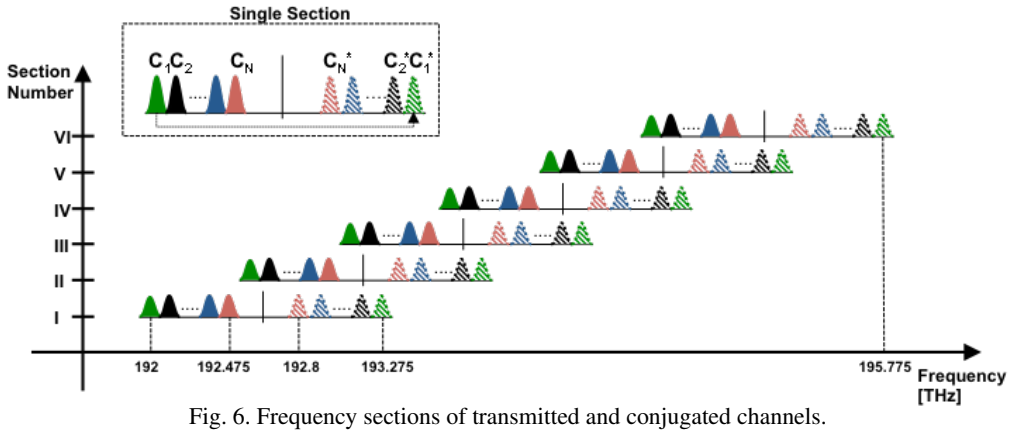

Fig. 6. Frequency sections of transmitted and conjugated channels.

The asymmetry between transmitted and conjugated channels (inter-span asymmetry) was calculated through a modified version of the previously used in-span asymmetry formula ([26]) that accounts for the different signal power evolution in the two channels:

$$Asymmetry = \frac{\int_0^L |P_1(z) - P_2(L-z)|dz}{\int_0^L P_1(z)} \times 100 \quad (2)$$

Optics EXPRESS

where L is the span length, P_1 and P_2 represents average signal power evolution of the transmitted and conjugated channels, respectively.

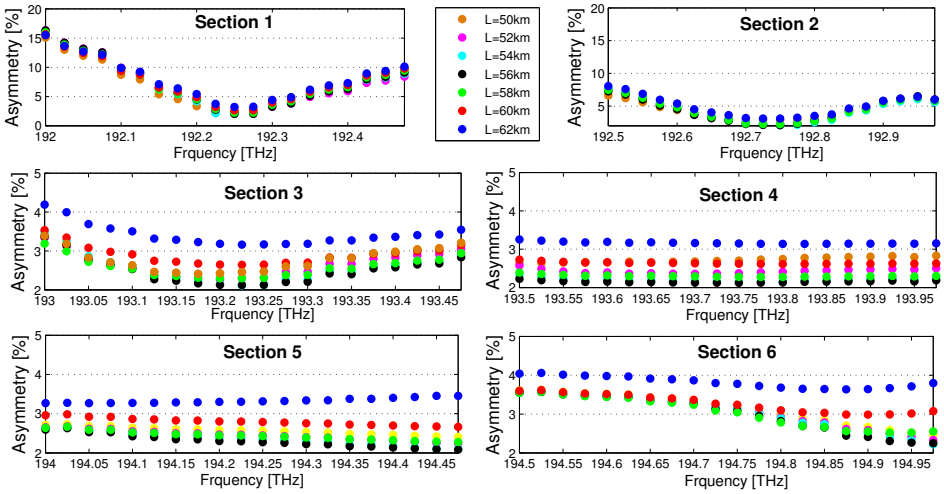

Fig. 7. Optimized asymmetry between transmitted and conjugated WDM channels at different frequency sections. The X axes refers to frequencies of the transmitted WDM grid.

Each section of the band was optimized to the channel that gave the best overall asymmetry performance: the grid was simulated to give 0 dB net gain for the first channel, then the rest of the channels were simulated with the same pump power, next we optimized the grid to a second channel and so on. The same logic was applied to the conjugated copy and finally we compared the asymmetry between original and conjugated channels with all possible combinations. The optimized results with the lowest achievable asymmetry in each section for the distances from 50 to 62 km links is shown in Fig. 7. Due to the frequency dependence of the attenuation and Raman gain coefficient profiles, the asymmetry in the residual windows (I and II) is most pronounced. This is also valid for single channel in-span asymmetry as shown in Fig. 4(a). As a result, the symmetry between transmitted and conjugated channels is greatest for the sections with the best in-span symmetry. Asymmetries below 4% are found to be achievable for all frequency sections from 193 - 195.775 THz (window III, IV, V and VI) at all span lengths considered.

Comparing the results from Fig. 7 we can notice the importance of span length optimization for wide band WDM transmission with OPC. A span length difference of only 4 km can lead to a strong performance decrease in nonlinear compensation using OPC due to the associated increase in asymmetry.

5. Conclusion

We have evaluated, for the first time, the signal power asymmetry between transmitted and conjugated channels in a WDM transmission in Raman-amplified systems with mid-link OPC. We have shown that for the chosen typical fiber-based OPC characteristics and a 20-channel, 25 GHz-spaced grid, a 56 km span length provides the most suitable solution that gives the best asymmetry performance, with values below 3% across most of the C-band. In terms of optimal channel location, the spectral window starting in 193.5 THz (window IV) offers the best possible performance for all span lengths studied.

Funding

Marie Skłodowska-Curie IF CHAOS for P. Rosa (658982); FP7 ITN programme ICONE (608099); Spanish MINECO grant ANOMALOS (TEC2015-71127-C2); Comunidad de Madrid grant SINFOTON (S2013/MIT-2790-SINFOTON-CM).